Research Square

Preprints are preliminary reports that have not undergone peer review.
They should not be considered conclusive, used to inform clinical practice,
or referenced by the media as validated information.

Rapid rise in the global ocean carbon sink determined from atmospheric oxygen observations

Elena Kozlova
e.kozlova@exeter.ac.uk

University of Exeter

Andrew Manning
University of East Anglia https://orcid.org/0000-0001-6952-7773

Ralph Keeling
University of California, San Diego https://orcid.org/0000-0002-9749-2253

Martin Heimann
Max-Planck-Institute for Biogeochemistry https://orcid.org/0000-0001-6296-5113

Yasunori Tohjima
National Institute for Environmental Studies

Sönke Zaehle
Max Planck Institute for Biogeochemistry

Andrew Watson
University of Exeter https://orcid.org/0000-0002-9654-8147

Physical Sciences - Article

Keywords:

Posted Date: June 7th, 2024

DOI: https://doi.org/10.21203/rs.3.rs-4473475/v1

License: This work is licensed under a Creative Commons Attribution 4.0 International License.
Read Full License

Additional Declarations: There is **NO** Competing Interest.

Rapid rise in the global ocean carbon sink determined from atmospheric oxygen observations

E. Kozlova[1], A. C. Manning[2], R. F Keeling[3], M. Heimann[4], Y. Tohjima[5], S. Zaehle[4], A. J. Watson[1]

1. Faculty of Environment, Science and Economy, University of Exeter, Exeter EX4 4QE UK

2. Centre for Ocean and Atmospheric Sciences, School of Environmental Sciences, University of East Anglia, Norwich NR4 7TJ, UK.

3. Scripps Institution of Oceanography, UC San Diego, La Jolla, Ca 92093, USA

4. Max Planck Institute for Biogeochemistry, 07745 Jena, Germany

5. National Institute for Environmental Studies, Tsukuba 305-8506, Japan

Abstract:

The rate of increase of atmospheric carbon dioxide (CO_2) in recent decades is only about half that expected if all anthropogenic emissions had stayed airborne. The "missing" CO_2 is absorbed by the oceans and land vegetation[1]. Of these two sinks for CO_2, the ocean sink is considered to be the better constrained[2-4]. Nevertheless, estimates of ocean uptake, using data products that integrate surface ocean observations[5-9], suggest a sink that is larger, and increasing more rapidly since about 2000, than do global ocean models, so that they now disagree substantially[1]. Here we examine the recent history of the CO_2 sinks using atmospheric observations of CO_2 and oxygen/nitrogen ratios from globally distributed measurement locations[10-12]. These provide a robust and independent separation of the ocean and land contributions. This method indicates that the ocean sink increased rapidly through the years 2000-2015, to values consistent with, though generally larger than, the surface-ocean based data products, but inconsistent with models. Since 2015, our results suggest this increase has stalled, but it remains 50% higher than most models predict.

Main

The rise in atmospheric carbon dioxide (CO_2) concentrations due to anthropogenic sources is considerably slowed by net uptake by the oceans and land vegetation, which together remove about half the amount of CO_2 emitted[1,13] The total of these sinks for CO_2 is well constrained, since it is the difference between the CO_2 emitted by fossil fuel combustion and the amount accumulating in the atmosphere, both of which are known with reasonable accuracy[1,14,15]. However, how much of the removed CO_2 goes into the land and how much to the ocean is less certain. In particular the ocean sink, which is the less variable term and is traditionally assumed to be better determined, is currently under scrutiny [9,16-18]. The Global Carbon Project (GCP) which publishes an annual accounting of the carbon budget, uses ensembles of both ocean biogeochemical models (OBGMs) and data products based on surface ocean observations to calculate this term[1]. These two methods show steady divergence over the last two decades, with the observation-based estimates increasing faster than the models. The average of the data products for the CO_2 flux into the ocean now exceeds the model average by about 0.8 petagrams of carbon per year (PgC yr^{-1}), which is around one third of the total ocean sink[1]. Both of these methods however have their limitations: the models have relatively coarse spatial resolution and rely on simplified physics and biology[16], whereas the data products are based on observations that are sparse and unevenly distributed in space and time, requiring extensive interpolation using machine learning or regression techniques[5]. For these reasons, an independent estimate of the ocean and land sinks is desirable.

High precision measurements of atmospheric O_2/N_2 ratios provide such an independent estimate of net land and ocean carbon sinks[11]. The method takes advantage of the fact that the net uptake of CO_2 by land vegetation is due to photosynthesis and releases oxygen, whereas uptake of CO_2 by the oceans does not have a similarly anticorrelated O_2 flux. A complication is that since the method was first proposed, it has become clear that the oceans are losing dissolved oxygen due to ocean warming, resulting in a net O_2 source to the atmosphere. The technique has been refined to account for this source of O_2[19], and to use the tracer atmospheric potential oxygen (APO)[20], a combination of O_2/N_2 and CO_2 measurements defined so that it is invariant to photosynthesis and therefore less subject to local interference sources. We use this method here, applied to the much larger number of atmospheric time series now available.

Calculation of atmospheric potential oxygen from time series observations.

We use flask sample observations from analyses made at three laboratories: Scripps Institution of Oceanography (SIO) in the USA[10], the National institute for Environmental Studies (NIES) in Japan[21], and the Max Planck Institute for Biogeochemistry (MPI-BGC) in Germany[22]. These laboratories report atmospheric CO_2 mole fractions and O_2/N_2 ratios from 21 fixed stations, as well as an extensive network of ship observations in the Pacific operated by NIES (Figure 1). Further details of the data sources and the stations are in Table 1 in the Methods section.

Oxygen measurements are reported as $\delta(O_2/N_2)$ ratios, in units of per meg [11]. Since dry air

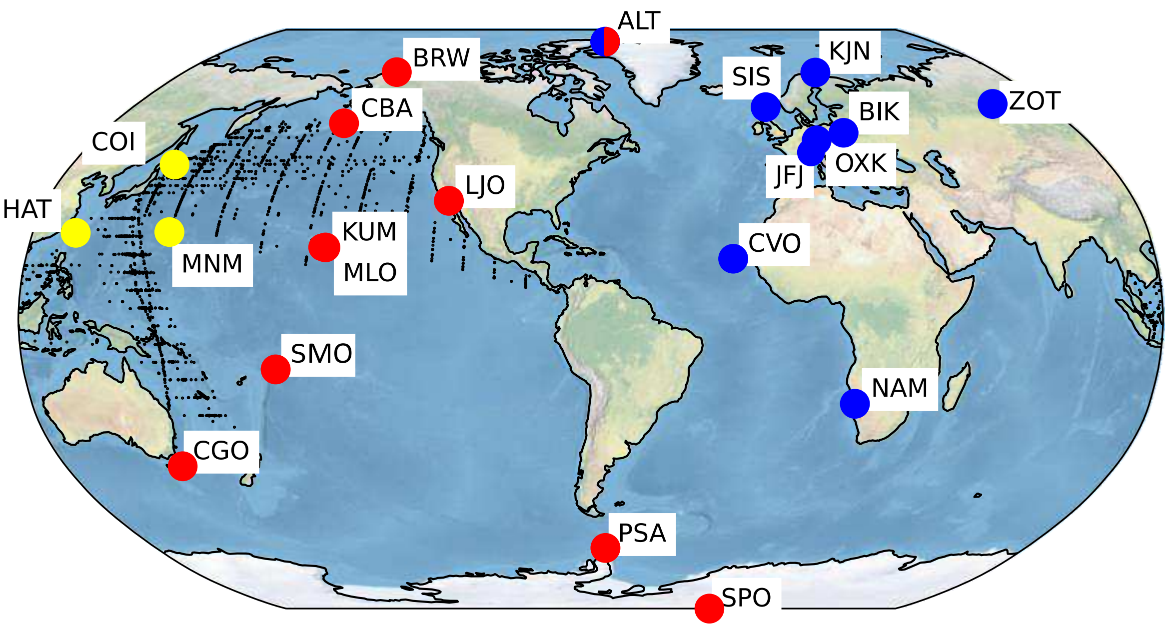

Figure 1: Locations of the fixed stations carrying out $\delta(O_2/N_2)$ sample collection (Red – SIO, Blue – MPI-BGC, Yellow – NIES) and of ship-based sampling operated by NIES (small black dots). Details of the stations are given in Table I of the Methods.

consists of about 21% oxygen, a change of one micromole of oxygen per mole of air is equivalent to about $(0.21)^{-1}$ or 4.8 per meg. The different laboratories use distinct calibration scales, and we have therefore adjusted all O_2 data to the SIO2017 O_2 scale (see Methods). With these adjustments, we calculated a δAPO value for each observation of XCO_2, the CO_2 mole fraction, and $\delta(O_2/N_2)$ according to the equation of Manning and Keeling[19]:

$$\delta\text{APO}=\delta(O_2/N_2) + \frac{\alpha_B}{XO_2}(XCO_2 - 350) \quad \text{(i)}$$

Here, α_B is the average molar ratio of O_2 released to CO_2 absorbed during land photosynthesis, assumed to be the same as the ratio of CO_2 released to oxygen absorbed in terrestrial respiration, this parameter is taken to be 1.1 +/- 0.05, and XO_2 = 0.209436, the approximate molar ratio of O_2 in dry air, inherent to the SIO2017 calibration scale. 350 is an arbitrary value of the SIO scale.

The δAPO and CO_2 flask data records for individual stations, and the ship data after grouping into ten-degree latitude bands, were curve-fitted as described in the Methods section to obtain representations of the seasonal cycles and the de-seasonalized rate of change at each site. The procedure included a low-pass filter with a gaussian kernel having a 40-day half-width, short enough to retain the inter-annual variations in the rate of change.

Global rate of decline of atmospheric potential oxygen

δAPO is defined to be invariant to the land sink. It is however declining in the atmosphere due to fossil fuel combustion and the removal of CO_2 by the ocean without a corresponding release of oxygen. We therefore seek to define a rate of change of δAPO appropriate to the atmosphere as a whole.

Figure 2 shows rates of change of δAPO calculated over five-year periods from 1990 to 2020 from each of the stations and latitudinal ship averages. For each station the rates of change were constructed by first calculating annual averages by integrating the smoothed curve fits from the start to the end of each year, then fitting a continuous, piece-wise linear function with hinge points at 1995.0, 2000.0, … 2015.0 to those annual averages (see Methods). Values are only shown for stations where an annual average could be calculated for every year in a given 5-year interval. Rates of decline increase with time, and are somewhat location dependent, but for periods after 2000, the agreement between the stations is quite good. The standard deviation of the stations for each 5 year period after 2000 ranges from 0.45-0.60 per meg per year, which is only about 5% of the rate of decline.

To construct a trend for the atmosphere as a whole, we created a representation for δAPO in the marine boundary layer as a function of latitude and time. For this we used only the stations near the ocean and near sea level (see Table I in Methods), except for the South Pole. The smoothed curves of the individual stations and latitudinal ship averages were sampled at regular intervals of 0.1 years and 4th-order polynomial functions of the sine of latitude fitted to these samples at each time slice. The result is a “flying carpet” plot as a function of latitude and time (Figure 3). This 3-D surface was then integrated with latitude over the area of the Earth’s surface, to give a representative time series for global mean surface δAPO.

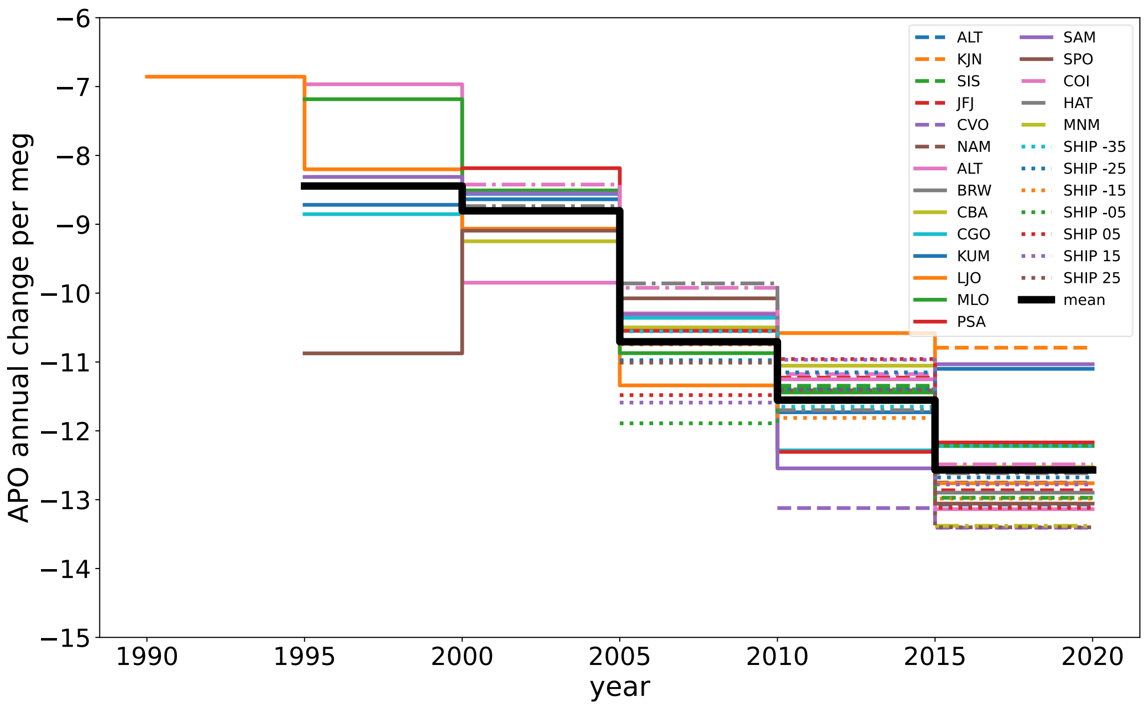

Figure 2: Rates of change of δAPO for individual stations and latitudinally averaged ship data, averaged over five-year intervals 1990-1995, 1995-2000, etc up to 2015-2020. Individual stations are distinguished by different colours and identified by their three-letter codes. SIO stations are solid lines, MPI-BGC stations are dashed lines and NIES stations are dot-dash lines. The latitudinally binned NIES ship data are dotted lines, identified by the central latitude between 25°N and 35°S. The black line is an unweighted mean of all stations and ship data in each 5-year period.

Ocean oxygen outgassing

An estimate of this flux is needed in order that the atmospheric observations can be used to quantify the ocean and land CO_2 sinks. Deoxygenation of the ocean is driven by several mechanisms related to climate warming and global change[23]. The solubility of O_2 in water decreases with increasing temperature, which will drive a direct loss of O_2 from surface waters to the atmosphere due to ocean warming. In addition, the ventilation of deeper water is expected to reduce as the oceans become more vertically stratified, resulting in less uptake of oxygen in temperate and cold regions. It has also been shown that some plankton communities are stimulated to fix more carbon as CO_2 partial pressure rises[24]. These processes lead to reduced uptake or greater release of oxygen in surface waters, with corresponding depletion at depth. Over recent decades, the uptake and release of oxygen by

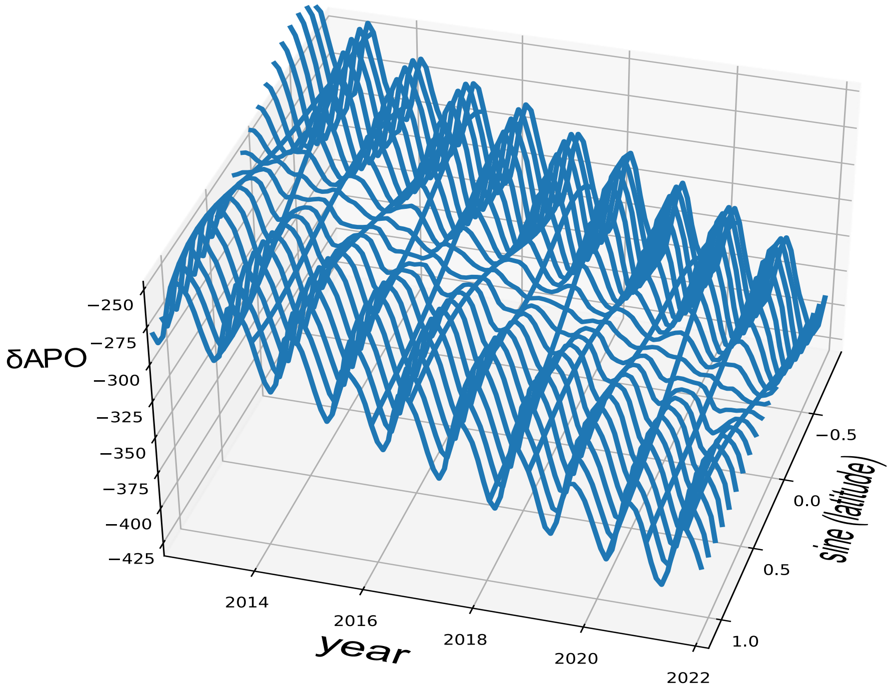

Figure 3: Wireframe representation of δAPO (in per meg) in the marine boundary layer as a function of time and latitude. The northern and southern hemispheres are dominated by seasonal cycles with maxima in the summer, which inter-leave in the equatorial regions. Only the last 12 years are shown, to better show the structure.

the ocean are expected therefore to be significantly out of balance with a net source to the atmosphere.

Keeling and Garcia[25] used the relationship between ocean heat uptake and degassing of oxygen as a proxy for O_2 outgassing. Ito et al[26] confirmed that the rate of loss of O_2 in the top 1000 m of the ocean is closely tied to ocean heat uptake, deriving a linear relationship of 8.2 +/- 0.7 nmol O_2 per joule of heat gained. The surprisingly tight correlation suggests that this O_2 loss is closely related to interaction with the atmosphere, so it is likely that this oxygen is escaping at the surface into the atmosphere. We used their result to quantify the O_2 flux out of the ocean from heat uptake data. Annual estimates of heat uptake averaged over 5 yearly periods presented in Figure 2 were calculated from the Levitus World Ocean Atlas (WOA) estimates[27]: https://www.ncei.noaa.gov/data/oceans/.

The rate of loss of upper ocean O_2 calculated by this method for the years 1990 to 2020 is 65 Tmol yr^{-1}, with year-to-year standard deviation of 33 Tmol yr^{-1}. For comparison, the decline of global ocean O_2 from 2004-2022 found in the recently published GOBAI data product for marine oxygen concentrations is 45±5 Tmol yr^{-1} over the upper 1000m, or 84±2 Tmol yr^{-1} over the upper 2000m[28] (calculated from Table B5 of that publication). These are estimates of O_2 deoxygenation in the ocean interior, which is not necessarily equivalent to outgassing to the atmosphere, however the global O_2 flux out of the ocean cannot at present be reliably calculated using surface observations alone. An estimate is available from ECCO-Darwin, a state estimation of ocean physics and biogeochemistry which assimilates both physics and biogeochemical data, which gives a value of 62 Tmol yr^{-1} for the period 1994-2017[28].

To reflect the large uncertainty on the ocean outgassing term we assigned a 1-σ value of 25 Tmol yr^{-1} to this flux, implying that with ~95 % confidence (i.e. 2-σ) the flux lies between 15 and 115 Tmol yr^{-1}. This is the largest uncertainty in the calculation of the ocean sink (Table S3 in the supplementary information gives contributions of all the uncertainties considered). Uncertainty on the land sink is larger than that of the ocean sink because it is more sensitive to errors in the total amount of fossil fuel CO_2 emitted.

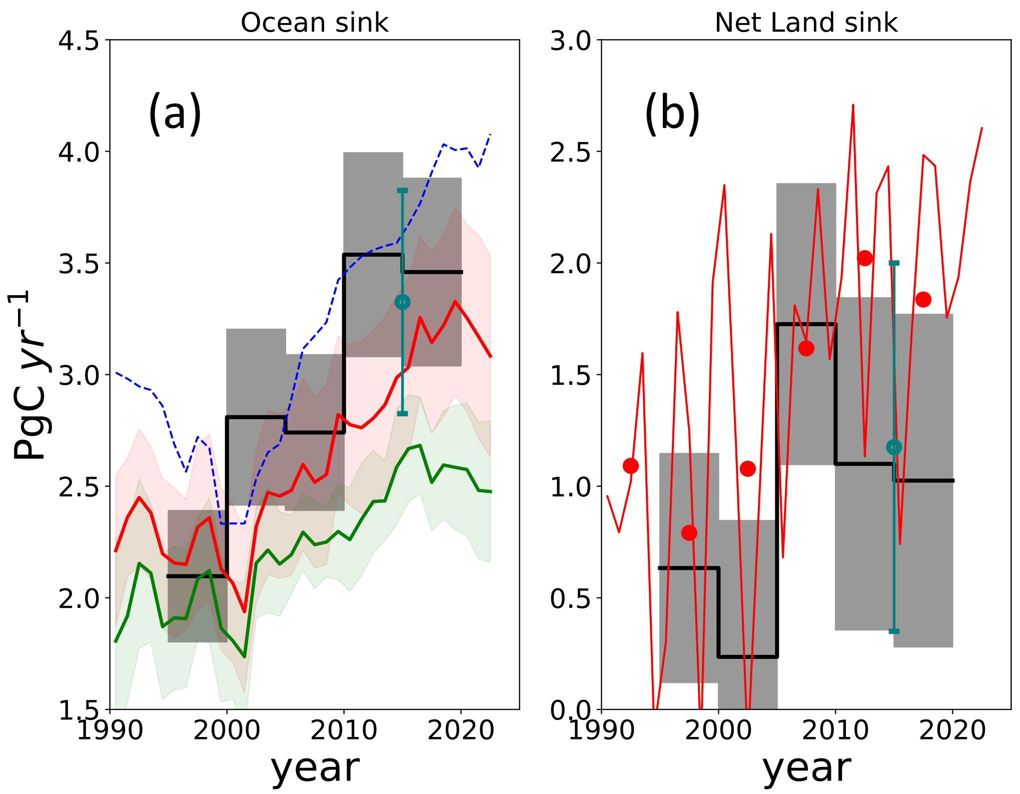

Figure 4: (a) Ocean and (b) net land carbon sinks (black lines) calculated from δAPO and CO_2 trends in the atmosphere averaged over 5-year periods, with 1-σ uncertainties (grey bands). The data sources, and equations from Manning and Keeling, are given in the Methods. Coloured lines: sink estimates from the Global Carbon Project budgets[1]: For the ocean sink, green is the mean of GCP ocean models, red is the mean of surface ocean CO_2 data products, with colour shading showing the standard deviations of the individual submissions. The blue dashed line is a data product (not included with the others) using surface ocean data corrected for skin temperature variations in the very near surface[9]. For the land sink the GCP estimate (red lines) and its 5-year average (red dots) are shown. The teal-coloured data point on each plot is the estimate from the 2023 global carbon budget for the 2010-2020 decade[1], using the O_2/N_2 method based on three stations only.

CO_2 sink estimates

Figures 4a and b show our best estimates for the ocean and net land sinks for atmospheric CO_2, respectively, calculated using the marine boundary layer δAPO product shown in Figure 3, integrated annually and over the Earth's surface. The sinks have been calculated as means for each five-year period between 1995 and 2020: numerical values are given in the Supplementary information. The grey shading shows 1-σ uncertainties calculated from 100 Monte-Carlo runs using randomly chosen parameters from gaussian uncertainty distributions (see Methods). Since any definition for the global atmospheric average concentration derived from a set of individual stations is open to question, we also repeated the calculations with the change in δAPO taken as the mean of the stations shown in Figure 2, and the standard deviation of the stations as the uncertainty (see Figure S1 in the supplementary Information). This deliberately simplistic approach makes no attempt to weight the stations to represent regions of the atmosphere. However, the results are similar to those of Figure 4, and within 1-σ bounds. This suggests that the method used to combine the station data to produce a global estimate of APO is not crucial to the results.

Also shown in Figure 4 are sink estimates from the GCP[1]. For the ocean sink we show values from the average of ocean models, the average of surface ocean data products, and a data product (not included in that average) that accounts for near-surface skin effect temperature variations, which significantly increases the flux. The GCP net land sink estimates are highly variable from year to year, (red line) so for better comparison we also show 5-year averages (red dots). The most recent global carbon budget includes an estimate for the two sinks by the O_2/N_2 method for the decade of 2010-20, also shown in the figure, which however uses only three stations as distinct from the 25 records used here; nevertheless, the estimate for this decade is similar to ours.

The O_2/N_2 method suggests a rapidly increasing ocean sink for the period from 1995 to 2015. It suggests a value consistent with the upper end of the data products, indeed, it most closely matches the data product that takes into account skin temperature effects and is substantially larger than the others. By contrast, it does not match the ocean model estimates well. However, the O_2/N_2 method suggests the rapid increase did not continue after 2015, unlike the data products (which continue to increase throughout the decade of the 2010s) and more in accord with the trend of model estimates for that period.

Conclusions

The good number of stations with O_2/N_2 observations now available give a coherent view of the rate of change of oxygen in the atmosphere, which translates comparatively directly into estimates of the ocean sink for anthropogenic CO_2. Uncertainties are on the order of 0.45 PgC yr^{-1} (1- σ) when integrated over five year periods, with errors in estimating the outgassing of oxygen from the ocean making the largest contribution. The values obtained for the ocean sink are broadly consistent with observational approaches used by the Global Carbon Project and by their models before 2000 (which is not surprising, as models were originally adjusted[3] to be consistent with estimates of the ocean sink[29] compatible with results from the O_2/N_2 method at that time[19]. However, our results indicate a more rapid increase of the ocean sink than do models through the period up to 2015, with the ocean sink in recent years substantially greater than models suggest. Data products based on the gas exchange equation and surface ocean CO_2 observations are more consistent with the O_2/N_2 results up to 2015, with the O_2/N_2 method supporting values towards the higher end of the values given by those estimates.

The period of 2000-2015 includes the densest coverage of surface ocean carbon observations[30], during which we might expect calculations of the CO_2 ocean sink based on observations (as in the data products shown in Figure 4a) to be at their most reliable - before that time coverage is quite limited. This is also the period when the rate of increase of the ocean sink in the data products agrees best with the O_2/N_2 method. Since 2015, the coverage of these primary data has declined substantially. The pCO_2 data products are reliant on the use of machine learning techniques to interpolate the carbon observations to assist in filling in the always-sparse primary carbon data. Poor data coverage over extended periods is however not readily visible in the final data products, and there is a concern that they may tend to extrapolate past well-observed changes into the less-well-observed near-past and present. This might help to explain at least some of the recent discrepancy in trends diagnosed from $\delta(O_2/N_2)$ and surface pCO_2 observations. To help resolve the ongoing uncertainties about the fate of anthropogenic CO_2 these long-term observation programmes, both in the atmosphere and oceans, need to be supported and continued.

Methods

Sources of O_2/N_2 and CO_2 flask data

The earliest observations were begun by SIO in 1989, and through most of the 1990s all the available O_2/N_2 observations we use are from their network only. The number of observations increased greatly by 2000 with the commencement of the NIES program in the Pacific, while in the 2000s they were joined by observations in the Atlantic sector made by MPI-BGC.

Bi-monthly averaged data for $\delta(O_2/N_2)$ and XCO_2 from flasks, from the network operated by Scripps Institution[10,19] were downloaded from the UCSD site in May 2023. The archive 2022-12-02 was used: https://library.ucsd.edu/dc/object/bb56403139.

Flask data for $\delta(O_2/N_2)$ and XCO_2 from the MPI-BGC at Jena, Germany[22] were obtained from the archive maintained by MPI-BGC: https://doi.org/10.17617/3.ZQX1LI. We used the values calculated after correcting O_2/N_2 ratios for micro-leaks during flask storage, using the observed Ar/N_2 ratios[22].

Flask data for $\delta(O_2/N_2)$ and XCO_2 for the stations and ship-based sampling network operated by the National Institute for Environmental Studies [12,21] was downloaded from the Global Environmental Database, https://db.cger.nies.go.jp/ged/en, in September 2023.

δAPO was calculated for each record using equation (i) in the text.

The $\delta(O_2/N_2)$ and XCO_2 records, their locations and date of the start of the record are shown in Table I. The records all continue until January 2020 or beyond.

Table 1: Stations having records of $\delta(O_2/N_2)$ and XCO_2 in flask samples of air, and their use in our calculations.

Institute	Station	ID	Lat(N)	Lon(E)	Record starts (decimal year)	Used for MBL product (fig3)?	Used for fig 2?
MPI-BGC	Alert	ALT	82.45	-62.51	2005.3	Yes	Yes
MPI-BGC	Kjølnes	KJN	70.85	29.22	2014.8	No	Yes
MPI-BGC	Zotto	ZOT	60.8	89.35	2006.8	No	No
MPI-BGC	Shetland	SIS	59.85	-1.28	2005.3	Yes	Yes
MPI-BGC	Białystok	BIK	52.23	23.03	2005.9	No	No

MPI-BGC	Ochsenkopf	OXK	50.03	11.81	2007.1	No	No
MPI-BGC	Jungfraujoch	JFJ	46.55	7.98	2008.0	No	Yes
MPI-BGC	Cape Verde	CVO	16.85	-24.69	2007.3	Yes	Yes
MPI-BGC	Namibia	NAM	-23.56	15.05	2013.6	Yes	Yes
Scripps	Alert	ALT	82.45	-62.51	1989.9	Yes	Yes
Scripps	Barrow	BRW	71	-156	2010.9	Yes	Yes
Scripps	Cold Bay	CBA	55	-163	1995.6	Yes	Yes
Scripps	Cape Kumukahi	KUM	20	-155	1993.5	Yes	Yes
Scripps	La Jolla	LJO	33	-117	1989.4	Yes	Yes
Scripps	Mauna Loa	MLO	20	-156	1991.0	No	Yes
Scripps	American Samoa	SMO	-14	-170	1993.5	Yes	Yes
Scripps	Cape Grim	CGO	-41	150	1991.0	Yes	Yes
Scripps	Palmer Station	PSA	-65	-64	1996.7	Yes	Yes
Scripps	South Pole	SPO	-90	0	1991.9	Yes	Yes
NIES	Cape Ochiishi	COI	43.2	145.5	1998.9	Yes	Yes
NIES	Hateruma Island	HAT	24.1	123.8	1997.6	Yes	Yes
NIES	Minamitorishima	MNM	24.3	154.0	2011.8	Yes	Yes
NIES	Ship data		-35 – 45	130-240	2001.8	Yes	Yes

Adjustments to the O_2/N_2 scales

NIES data and MPI-BGC data were adjusted to bring them onto the SIO 2017 scale, as follows:

NIES O_2/N_2 data: A comprehensive intercomparison study by Aoki et al[31] of O_2/N_2 calibrations determined linear relationships between SIO and NIES scales. We used the data they provide (their table 4) to adjust the NIES data also to the SIO scale. In addition, we applied a drift in the offset of 0.28 per meg per year for the period since March 2010, which Rödenbeck et al [32] report is obtained by a linear fit to differences between regular simultaneous samples collected at La Jolla, San Diego, since that time.

MPI-BGC O_2/N_2 data: We used the O_2/N_2 data after “Argon correction” as reported by Heimann et al[22]. MPI-BGC data are calibrated to a scale referenced to the version of the SIO scale current in 2007. Figure S2 in the supplementary information shows a comparison of the flask records from Alert, during the period since 2005 when both SIO and MPI-BGC report flask observations there. There is good agreement but a systematic offset, which from 2005 to early 2015 and after early 2020 averages about 6.9 per meg, but in the intervening time is higher, about 13.4 per meg. Rödenbeck et al[1] provide a discussion of these offsets and conclude that a micro-leak in the measurement system caused the enhanced offset between 2015 and 2020. To align the MPI-BGC data with the current SIO scale, we applied the larger offset between March 2015 and May 2020, and the smaller offset to the remainder of the data.

Curve fitting the $\delta\mathrm{APO}$ time series of individual stations

Curve fitting to the $\delta\mathrm{APO}$ time series was performed on the fixed stations and also on the ship-based observations after grouping into ten-degree latitude bands. Using least squares regression, a curve with three harmonics to represent the seasonal cycle and a cubic polynomial to represent the annual trend was fitted to the $\delta APO_{\mathrm{data}}$ records as follows:

$$\delta APO_{model} = a_0 + \sum_{i=1}^{3} a_i t^i + \sum_{f=1}^{3}\left(b_f sin(2\pi f t) + c_f \cos(2\pi f t)\right) \qquad \text{(ii)}$$

Where a_0, a_i, b_f and c_f are constants found by the fitting procedure and t is time in years. The residuals of the data from the model ($\delta APO_{\mathrm{data}}$ - δAPO_{model}) were input to a low pass filter with a Gaussian kernel and a 40-day half-width at half height. Finally, this residual curve was added to the δAPO_{model} to produce a smoothed record that captures the lower frequency seasonal and annual variability of the data. For gaps in the time series longer than 200 days, a gap was left in the smoothed record, except in the case of the LJO record which has a substantial gap in 1990. This was filled by linear interpolation, since no other station was operating at that time. Figures S4-S29 show the 19 station time series and seven latitude-averaged groups of ship observations with the smoothed curve fits.

Other data sources

The Excel spread sheet linked to the Global Carbon Budget 2023[1] was the source of data on the annual release of CO_2 from coal, oil, natural gas and cement-production since 1990, and the burden of CO_2 in the atmosphere. We used values for the O_2/ CO_2 stoichiometry of these processes as quoted by Keeling and Manning[10].

Calculation of sinks

We used the equations for the ocean sink (O) and the net land sink (L) given by Manning and Keeling[19], with the addition of a small correction term due to oxygen sources from industrial processes as recently complied by Battle et al[33]. The equations are:

$$O = \left[\left(-\Delta(\delta\mathrm{APO}) \times M_{atm} \times X_{O_2} \times m_c\right) + \alpha_B \times F - FOD + \left(Z_{eff} + I\right) \times m_c\right] \times 1/\alpha_B$$

And

$$L = F - O - \Delta XCO_2 \times M_{atm} \times m_c$$

Where

$$Z_{eff} = Z - \Delta N_2 \times \frac{X_{N_2}}{X_{O_2}}$$

$$Z = H \times \frac{d[O_2]}{dH}$$

$$\Delta N_2 = H \times \frac{dS_{N_2}}{dT} \times \frac{1}{c_p}$$

Definitions are:

F = fossil fuel source in gC yr^{-1}.

FOD = oxygen demand of the fossil fuel source in moles per year multiplied by m_c (see below: also, effectively therefore in gC yr^{-1}).

$\Delta(\delta \mathrm{APO})$ is the change in δAPO in mole fraction per year.

ΔXCO_2 is the change in atmospheric CO_2 in mole fraction per year.

M_{atm} is the number of moles in the atmosphere.

m_c is the molecular weight of carbon (equals 12).

I is the number of moles of O_2 released by industry in a year[33].

Z is the moles of O_2 released from the ocean due to heating in a year. ΔN_2 is the moles of nitrogen released by heating in a year. Z_{eff} is the molar correction to the calculated ocean sink for these releases. *Z* is calculated as the product of *H*, the yearly uptake of heat by the ocean, and $\frac{dO_2}{dH}$, the rate of change of oxygen concentration in seawater with heat input (see discussion in text) while ΔN_2 is calculated as the product of $\frac{dS_{N_2}}{dT}$, the rate of change of N_2 solubility with temperature, and $1/c_p$ where c_p is the specific heat capacity of seawater. Table S4 in the supplementary information gives five-year-average values for *F, FOD*, Z_{eff} and *I*.

Constants are given in the table below.

Constant	Value
M_{atm}	1.77 x 10^{20} mol
$\frac{dS_{N_2}}{dT}$	1.03 x 10^{-5}mol $l^{-1}K^{-1}$ (at 288.15 K)
$\frac{d[O_2]}{dH}$	8.2 x 10^{-9}mol J^{-1}
X_{O_2}	0.20943 6
X_{N_2}	0.78084
C_p	4108 Joules $l^{-1}K^{-1}$

Smoothed model fits to Individual station records

The supplementary information file contains plots of δAPO for all the stations and latitudinally binned ship-based observations used in this study.

Sources of uncertainty

The Monte Carlo results in figure 4 include five sources of uncertainty. We assumed 1-sigma values as follows: (1) a 5% margin of error for the rate of fossil fuel emissions: (2) uncertainties in the ratio of O_2: consumed to CO_2 released by fossil fuel combustion, of 0.03-0.04 mol mol^{-1} for the major fuel types[10]; (3) a 5% uncertainty for α_B, the molar ratio of O_2 released to CO_2 taken up in land photosynthesis; (4) the uncertainty in the rate of decline of global δAPO, calculated from the fitting procedure when using the global surface product, or the standard deviation of individual stations when using the mean of stations; (5) the uncertainty in ocean outgassing of O_2 of 25 Tmol yr^{-1} as discussed in the main text.

The individual contributions of each these sources of uncertainty to the calculation of sinks, are given in Table S3 in the supplementary information. For the ocean CO_2 sink as shown in Figure 4a, ocean outgassing is the largest term, and error in the O:C ratio for combustion of coal, oil and gas fossil fuels is the next largest. The other terms have comparatively small influences on the ocean sink, but the fossil fuel uncertainty has a much larger effect on the calculation of the land sink. Overall the terms add in quadrature giving values of ~0.45 PgC yr^{-1} for the ocean sink and ~0.75 PgC yr^{-1} for the land sink.

Data and code availability

The atmospheric O_2/N_2 and CO_2 flask data are available from the data archives of the three primary data providers (SIO, NIES and MPI-BGC) at the URLs given above in the Methods Section. Data from the Global Carbon Budget is available from spreadsheets linked to those publications, at the ICOS Carbon Portal: https://www.icos-cp.eu/science-and-impact/global-carbon-budget/.

The python code used to process the data is available on request from the authors at U. Exeter.

Acknowledgements

EK and AJW thank the Royal Society for funding under Research Professorship grants RP140106 and RP\EA\180008, the UKRI for support under grant NE/S003606/1 and the UK government Horizon Europe Funding Guarantee, and the European Union under grant agreement no. 101083922 (OceanICU; https://ocean-icu.eu/). YT thanks Toshinobu Machida, Motoki Sasakawa, Yukio Terao, and Nakaoka Shin-ichiro for their continued support of NIES flask sampling and CO_2 measurements: NIES flask observations were financially supported by the Global Environmental Research Coordinate System from the Ministry of the Environment, Japan (grant nos. E0955, E1451). We thank A Jordan, W Brandt, Heiko Moossen and others for performing the flask analyses of CO_2 and O_2/N_2 ratios at MPI-BGC.

Author information

Contributions: Design by EK, AJW and ACM. Writing by EK and AJW with contributions from all authors. Data contributions from RFK, YT, MH, and SZ. Calculations and coding by AJW and EK.

References

1 Friedlingstein, P. *et al.* Global Carbon Budget 2023. *Earth Syst. Sci. Data* **15**, 5301-5369 (2023). https://doi.org:10.5194/essd-15-5301-2023

2 DeVries, T. *et al.* Magnitude, Trends, and Variability of the Global Ocean Carbon Sink From 1985 to 2018. *Global Biogeochemical Cycles* **37** (2023). https://doi.org:10.1029/2023GB007780

3 Le Quéré, C. *et al.* Trends in the sources and sinks of carbon dioxide. *Nature Geoscience* **2**, 831-836 (2009). https://doi.org:10.1038/ngeo689

4 Wanninkhof, R. *et al.* Global ocean carbon uptake: Magnitude, variability and trends. *Biogeosciences* **10**, 1983-2000 (2013). https://doi.org:10.5194/bg-10-1983-2013

5 Landschützer, P. *et al.* A neural network-based estimate of the seasonal to inter-annual variability of the Atlantic Ocean carbon sink. *Biogeosciences* **10**, 7793-7815 (2013). https://doi.org:10.5194/bg-10-7793-2013

6 Gloege, L., Yan, M., Zheng, T. & McKinley, G. A. Improved Quantification of Ocean Carbon Uptake by Using Machine Learning to Merge Global Models and pCO2 Data. *Journal of Advances in Modeling Earth Systems* **14** (2022). https://doi.org:10.1029/2021MS002620

7 Gregor, L. & Gruber, N. OceanSODA-ETHZ: A global gridded data set of the surface ocean carbonate system for seasonal to decadal studies of ocean acidification. *Earth System Science Data* **13**, 777-808 (2021). https://doi.org:10.5194/essd-13-777-2021

8 Rödenbeck, C., Devries, T., Hauck, J., Le Quéré, C. & Keeling, R. F. Data-based estimates of interannual sea-Air CO2 flux variations 1957-2020 and their relation to environmental drivers. *Biogeosciences* **19**, 2627-2652 (2022). https://doi.org:10.5194/bg-19-2627-2022

9 Watson, A. J. *et al.* Revised estimates of ocean-atmosphere CO2 flux are consistent with ocean carbon inventory. *Nature Communications* **11** (2020). https://doi.org:10.1038/s41467-020-18203-3

10 Keeling, R. F. & Manning, A. C. in *Treatise on Geochemistry: Second Edition* Vol. 5 385-404 (2014).

11 Keeling, R. F. & Shertz, S. R. Seasonal and Interannual Variations in Atmospheric Oxygen and Implications for the Global Carbon-Cycle. *Nature* **358**, 723-727 (1992).

12 Tohjima, Y., Mukai, H., MacHida, T., Hoshina, Y. & Nakaoka, S. I. Global carbon budgets estimated from atmospheric O2N2 and CO2 observations in the western Pacific region over a 15-year period. *Atmospheric Chemistry and Physics* **19**, 9269-9285 (2019). https://doi.org:10.5194/acp-19-9269-2019

13 2021, I. Climate Change 2021: The Physical Science Basis. Contribution of Working Group I to the Sixth Assessment Report of the Intergovernmental Panel on Climate Change 2391 (2021).

14 Andrew, R. M. A comparison of estimates of global carbon dioxide emissions from fossil carbon sources. *Earth System Science Data* **12**, 1437-1465 (2020). https://doi.org:10.5194/essd-12-1437-2020

15 Keeling, C. D., Bacastow, R. B. & Bainbridge, A. E. Atmospheric carbon dioxide variations at Mauna Loa Observatory, Hawaii. *TELLUS* **28**, 538-551 (1976). https://doi.org:10.3402/tellusa.v28i6.11322

16 Hauck, J. *et al.* Consistency and Challenges in the Ocean Carbon Sink Estimate for the Global Carbon Budget. *Frontiers in Marine Science* **7** (2020). https://doi.org:10.3389/fmars.2020.571720

17 Gray, A. R. *et al.* Autonomous Biogeochemical Floats Detect Significant Carbon Dioxide Outgassing in the High-Latitude Southern Ocean. *Geophysical Research Letters* **45**, 9049-9057 (2018). https://doi.org:10.1029/2018GL078013

18 Long, M. C. *et al.* Strong Southern Ocean carbon uptake evident in airborne observations. *Science* **374**, 1275-1280 (2021). https://doi.org:10.1126/science.abi4355

19 Manning, A. C. & Keeling, R. F. Global oceanic and land biotic carbon sinks from the Scripps atmospheric oxygen flask sampling network. *Tellus Series B-Chemical and Physical Meteorology* **58**, 95-116 (2006).

20 Stephens, B. B. *et al.* Testing global ocean carbon cycle models using measurements of atmospheric O2 and CO2 concentration. *Global Biogeochemical Cycles* **12**, 213-230 (1998). https://doi.org:10.1029/97GB03500

21 Tohjima, Y. *et al.* Analysis of seasonality and annual mean distribution of atmospheric potential oxygen (APO) in the Pacific region. *Global Biogeochemical Cycles* **26** (2012). https://doi.org:10.1029/2011GB004110

22 Heimann, M. J., A., Brand, W., Lavric, J, Moossen, H., and Rothe, M., . The atmospheric flask sampling program of MPI-BGC, Version 13, 2022. (Max Planck Insitute for Biogeochemistry, Jena, Germany, 2022).

23 Oschlies, A., Brandt, P., Stramma, L. & Schmidtko, S. Drivers and mechanisms of ocean deoxygenation. *Nature Geoscience* **11**, 467-473 (2018). https://doi.org:10.1038/s41561-018-0152-2

24 Riebesell, U. *et al.* Enhanced biological carbon consumption in a high CO2 ocean. *Nature* **450**, 545-548 (2007). https://doi.org:10.1038/nature06267

25 Keeling, R. F. & Garcia, H. E. The change in oceanic O2 inventory associated with recent global warming. *Proceedings of the National Academy of Sciences of the United States of America* **99**, 7848-7853 (2002). https://doi.org:10.1073/pnas.122154899

26 Ito, T., Minobe, S., Long, M. C. & Deutsch, C. Upper ocean O2 trends: 1958–2015. *Geophysical Research Letters* **44**, 4214-4223 (2017). https://doi.org:10.1002/2017GL073613

27 Levitus, S. *et al.* World ocean heat content and thermosteric sea level change (0-2000m), 1955-2010. *Geophysical Research Letters* **39** (2012). https://doi.org:10.1029/2012GL051106

28 Carroll, D. *et al.* The ECCO-Darwin Data-Assimilative Global Ocean Biogeochemistry Model: Estimates of Seasonal to Multidecadal Surface Ocean pCO2 and Air-Sea CO2 Flux. *Journal of Advances in Modeling Earth Systems* **12** (2020). https://doi.org:10.1029/2019MS001888

29 Denman, K. *et al.* Chapter 7, Climate Change 2007,: The physical Science Basis. Contribution of Working Group 1 to the fourth assessment report of the Intergovemmental Panell on Climate Change. 499-587 (2007).

30 Bakker, D. C. E. *et al.* A multi-decade record of high-quality fCO2 data in version 3 of the Surface Ocean CO2 Atlas (SOCAT). *Earth System Science Data* **8**, 383-413 (2016). https://doi.org:10.5194/essd-8-383-2016

31 Aoki, N. *et al.* Intercomparison of O2/N2ratio scales among AIST, NIES, TU, and SIO based on a round-robin exercise using gravimetric standard mixtures. *Atmospheric Measurement Techniques* **14**, 6181-6193 (2021). https://doi.org:10.5194/amt-14-6181-2021

32 Rödenbeck, C. *et al.* The suitability of atmospheric oxygen measurements to constrain western European fossil-fuel CO2 emissions and their trends. *Atmospheric Chemistry and Physics* **23**, 15767-15782 (2023). https://doi.org:10.5194/acp-23-15767-2023

33 Battle, M., Raynor, A., Kesler, S. & Keeling, R. The Impact of Industrial Activity on the Amount of Atmospheric O2. *Tellus B: Chemical and Physical Meteorology,* **75**, 65-75 (2023). https://doi.org:10.16993/tellusb.1875

Supplementary Files

This is a list of supplementary files associated with this preprint. Click to download.

- supplementaryinfoKozlovaetal.pdf